Supplementary Material Cover Sheet

Insights into the mechanisms of biochar-derived dissolved organic carbon-facilitated

transport of oxytetracycline in saturated porous media

Number of pages: 16

Number of tables: 3

Number of figures: 7

S1. Determination of the ζ-potential of sand grains

The zeta potential of sand grains was measured by using a zeta-plus potential analyzer (Zetasizer nano ZS90, Malvern Instruments, UK) at room temperature (25°C) according to the method described in previous studies.[1,2] It should be noted that the sand grains were too large for direct measurement by the zeta potential analyzer, a few sand grains were crushed into fine powders and then mixed with the appropriate chemistry solution (see Table 1) in an ultrasonic bath for 30 min. Then, the mixture formed a sufficiently stable suspension that could be used for zeta potential measurement. Note that the zeta potential was calculated from the electrophoretic mobility using the full numerical model by O'Brien and White.[3]

S2. Calculation of UV–vis indexes

Absorbance was measured using a TU-1810PC UV–vis spectrophotometer (Beijing Purkinje General Instrument Co., Beijing, China) within a spectrum of 250–700 nm, at 1-nm increments, using a 1-cm quartz cuvette. Samples were allowed to come to room temperature before measurements were taken. The absorption coefficient a (m^{-1}) was calculated for each wavelength (λ) using the equation:[4]

$a_{\lambda} = 2.303 A_{\lambda} /l$

where A_{λ} is the absorbance and l is the path length of the optical cell in meters (here $l = 0.01$ m). Measurements for the control were also subtracted after subtracting blank measurements.

$SUVA_{254}$ (L/(mg-C·m)) was calculated using the equation:
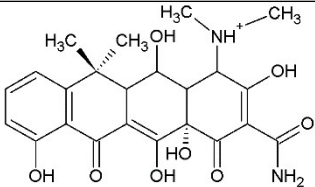
$SUVA_{254} = a_{254}/C_{BDOC}$

where a_{254} (m^{-1}) is the absorbance coefficient at 254 nm. C_{BDOC} (mg/L), the BDOC concentration in solution, is 10 mg/L here.

$S_{275–295}$, the spectral slope was determined by fitting an exponential decay model (Sigmaplot Version 11, 2008, Systat Software, Inc.) to the absorption coefficients within the spectra 275–295 nm.[4]

S3. Determination of the OTC concentration in the effluent

The OTC concentration in the effluent in each sample was measured after solvent extraction.[5,6] Specifically, 3 mL of each sample was taken into 10 mL centrifuge tubes with 0.5 mL 0.25 M NaH_2PO_4 and 0.5 mL acetonitrile. Then, the vials were shaken at 25 °C in the dark for 2 h. Afterward, the samples were sonicated for 45 min to free the antibiotics associated with BDOC, immediately filtered through 0.1 μm pore size polytetrafluoroethylene membrane for analysis. The concentration of OTC was analyzed directly by using a Waters high performance liquid chromatography system (HPLC, e2695, Waters Alliance) equipped with a symmetry reversed-phase C18 column (4.6 × 150 mm) using a UV/visible detector at a wavelength of 360 nm. Pre-experiment showed the mass recovery of extraction process was $97.3 \pm 1.5\%$.

Table S1. Selected properties of OTC.

Molecular formula	Chemical structure	Molecular weight (g/mol)	Solubility (g/L) [a]	Log K_{ow}[b]	pk_a[a]
$C_{22}H_{24}N_2O_9$		496.47	0.062	-0 .90	pK_{a1}=3.22 pK_{a2}=7.46 pK_{a3}=8.94

[a] Derived from Daghrir and Drogui.[7]

Table S2. Assignments of FTIR spectrum.[8,9]

Wavenumber	Assignments
3311~3494 cm^{-1}	H-bonded hydroxyl groups or amino groups
2854~2931 cm^{-1}, 1370~1458 cm^{-1}	aliphatic C–H
1500~1620 cm^{-1}	aromatic C=C
1700~1750 cm^{-1}	C=O of carboxyl, aldehyde, ketone, and ester groups
1103~1205 cm^{-1}	C–O or C-N
745~881 cm^{-1}	aromatic C–H or C=C-H

Table S3. ζ-potential values (mV) of sand grains under various conditions.

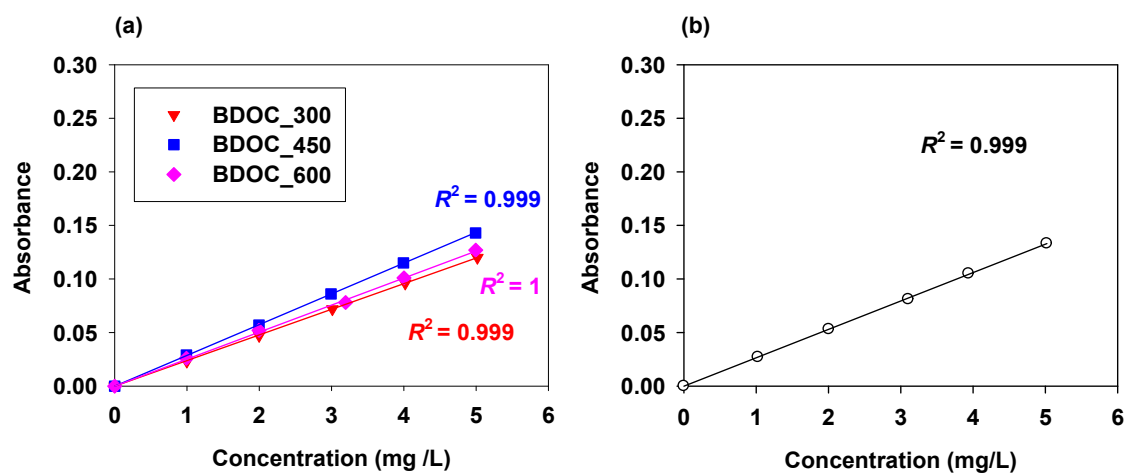| No.	Background solution	pH	ζ-potentials (mV)
1	10 mM NaCl	5.0	-32.7 ± 1.3
2	10 mM NaCl + BDOC_450	5.0	-35.3 ± 0.8
3	10 mM NaCl	7.0	-47.9 ± 1.1
4	10 mM NaCl + BDOC_300	7.0	-52.3 ± 0.5
5	10 mM NaCl + BDOC_450	7.0	-56.1 ± 0.7
6	10 mM NaCl + BDOC_600	7.0	-59.4 ± 1.2
7	10 mM NaCl	9.0	-55.1 ± 0.8
8	10 mM NaCl + BDOC_450	9.0	-58.7 ± 0.9
9	0.1 mM $CuCl_2$	5.0	-35.6 ± 0.5
10	0.1 mM $CuCl_2$ + BDOC_450	5.0	-42.6 ± 0.5

Fig. S1. Calibration curve as absorbance vs. concentration of (a) BDOC (absorbance at the wavelength of 430 nm) and (b) OTC (absorbance at the wavelength of 360 nm).
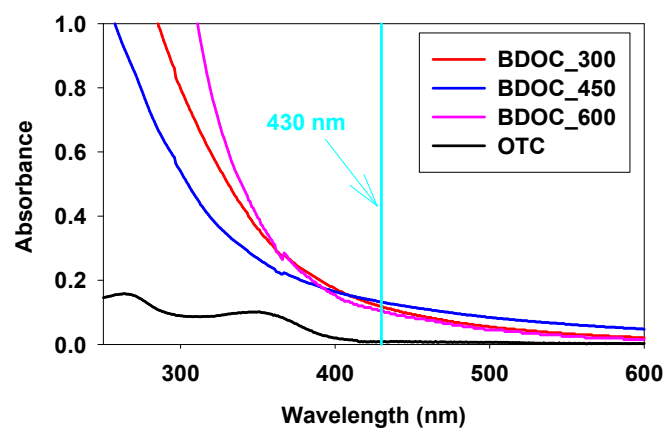
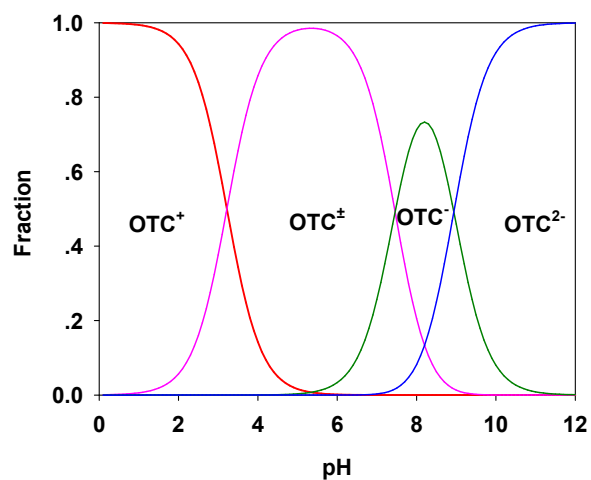**Fig. S2.** UV/Vis spectra of BDOC (5 mg/L) and OTC (5 mg/L) dispersed in DI water.

Fig. S3. pH-dependent speciation of the whole OTC molecular and the functional groups, respectively.
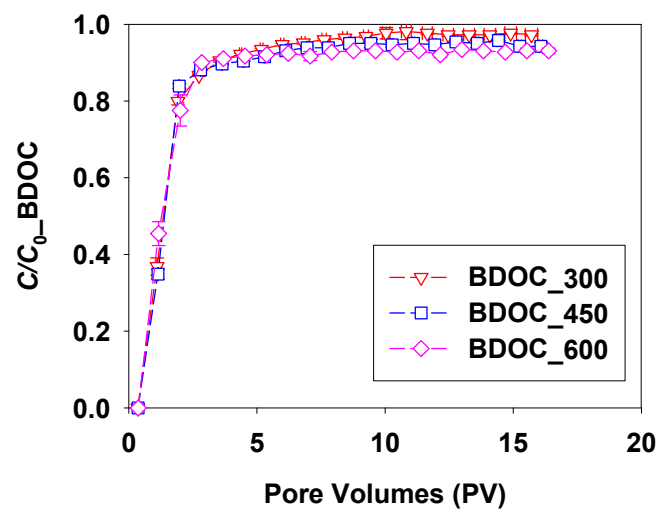
Fig. S4. Transport of different BDOC (10 mM NaCl at pH 7.0) in saturated sand columns.
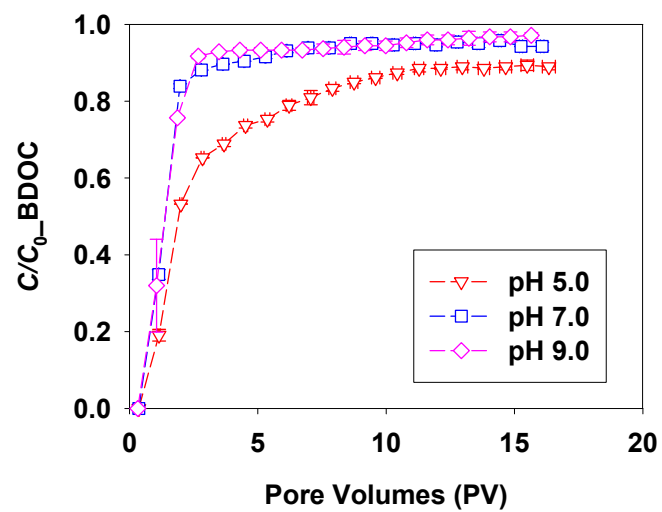
Fig. S5. Transport of BDOC in sand under different pH conditions (at 10 mM NaCl).
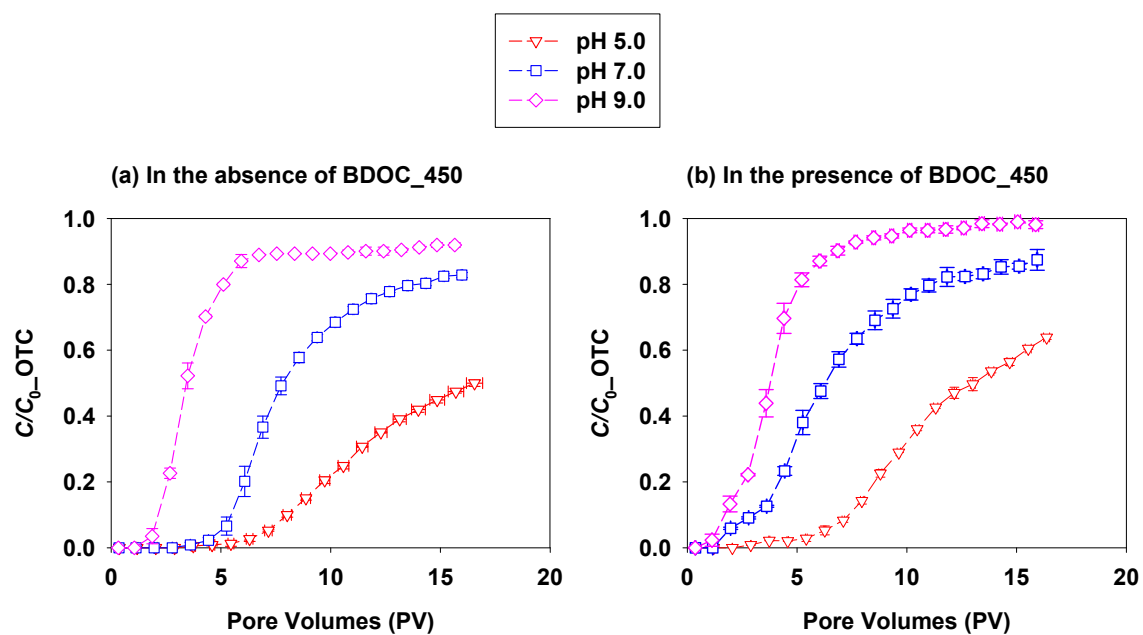
Fig. S6. Transport of OTC in sand under different pH conditions (at 10 mM NaCl): (a) in the absence of BDOC and (b) in the presence of BDOC.
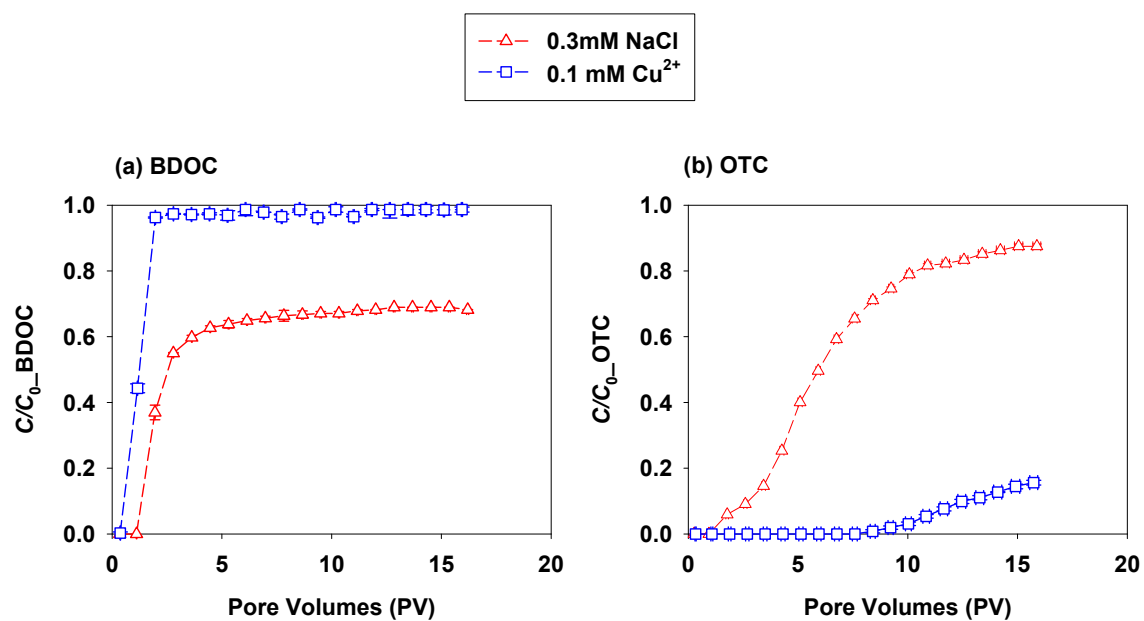
Fig. S7. Transport of (a) BDOC and (b) OTC in saturated sand in the presence of 0.3 mM Na^+ and 0.1 mM Cu^{2+} at pH 5.0.

References

1 C. V. Chrysikopoulos, N. P. Sotirelis, N. G. Kallithrakas-Kontos, Cotransport of Graphene Oxide Nanoparticles and Kaolinite Colloids in Porous Media, *Transp. Porous Media*, 2017, **119**, 181-204.

2 P. N. Mitropoulou, V. I. Syngouna, C. V. Chrysikopoulos, Transport of colloids in unsaturated packed columns: Role of ionic strength and sand grain size, *Chem. Eng. J.*, 2013, **232**, 237-48.

3 R. W. O'Brien, L. R. White, Electrophoretic mobility of a spherical colloidal particle, *J. Chem. Soc. Faraday Trans.*, 1978, **74**.

4 J. R. Helms, A. Stubbins, J. D. Ritchie, E. C. Minor, D. J. Kieber, K. Mopper, Absorption spectral slopes and slope ratios as indicators of molecular weight, source, and photobleaching of chromophoric dissolved organic matter, *Limnol. Oceanogr.*, 2008, **53**, 955-69.

5 K. X. Sun, S. N. Dong, Y. Y. Sun, B. Gao, W. C. Du, H. X. Xu, J. C. Wu, Graphene oxide-facilitated transport of levofloxacin and ciprofloxacin in saturated and unsaturated porous media, *J. Hazard. Mater.*, 2018, **348**, 92-9.

6 Y. N. Xing, X. J. Chen, X. Chen, J. Zhuang, Colloid-Mediated Transport of Pharmaceutical and Personal Care Products through Porous Media, *Sci. Rep.*, 2016, **6**.

7 R. Daghrir, P. Drogui, Tetracycline antibiotics in the environment: a review, *Environ. Chem. Lett.*, 2013, **11**, 209-27.

8 W. F. Chen, R. Wei, L. M. Yang, Y. S. Yang, G. P. Li, J. Z. Ni, Characteristics of wood-derived biochars produced at different temperatures before and after deashing:

Their different potential advantages in environmental applications, *Sci. Total Environ.*, 2019, **651**, 2762-71.

9 M. Keiluweit, P. S. Nico, M. G. Johnson, M. Kleber, Dynamic Molecular Structure of Plant Biomass-Derived Black Carbon (Biochar), *Environ. Sci. Technol.*, 2010, **44**, 1247-53.